Supplementary Information files for Insights into the structures adopted by titanocalix[6 and 8]arenes and their use in the ring opening polymerization of cyclic esters

Electronic Supplementary Information

Insights into the structures adopted by titanocalix[6 and 8]arenes and their use in the ring opening polymerization of cyclic esters

Orlando Santoro,[a] Mark R. J. Elsegood,[b*] Elizabeth V. Bedwell,[b] Jake A. Pryce,[b] and Carl Redshaw[a*]

[a] *Plastics Collaboratory, Department of Chemistry and Biochemistry, The University of Hull, Cottingham Rd, Hull, HU6 7RX, U.K.*

[b] *Chemistry Department, Loughborough University, Loughborough, Leicestershire, LE11 3TU, U.K.*

Contents

Figure S12. Side-on view of partial calixarene stacking in **10**.

Figure S13. Layers of molecules of **11** in the *a*/*c* plane.

Figure S14. ^{1}H NMR spectrum ($CDCl_3$, 400 MHz, 298 K) of the PCL synthesized in Table 1, entry 18.

Figure S15. MALDI-ToF spectrum of the PCL synthesized in Table 1, entry 16.

Figure S16. 2D *J*-resolved ^{1}H NMR spectrum ($CDCl_3$, 400 MHz, 298 K) of the PLA synthesized using [6]Ti_2Cl_3.

Figure S17 ^{13}C NMR spectrum ($CDCl_3$, 400 MHz, 298 K) of the CL-VL Copolymer synthesized with **10** (65-63 ppm)

Equation S1 Determination of number-average sequence length for CL.

Equation S2. Determination of number-average sequence length for VL.

Equation S3. Determination of the Randomness Character (*R*).

Figure S18 ^{13}C NMR spectrum ($CDCl_3$, 400 MHz, 298 K) of the CL-VL Copolymer synthesized with **11** (65-63 ppm)

Figure S19 ^{13}C NMR spectrum ($CDCl_3$, 400 MHz, 298 K) of the CL-VL Copolymer synthesized with **12** (65-63 ppm)

Figure S20 ^{1}H NMR spectrum ($CDCl_3$, 400 MHz, 298 K) of the crude ε–CL/*r*-LA co-polymerization mixture synthesized with **1**

Crystallographic experimental details.

The following section gives details of disorder and solvent of crystallization modelling for the individual crystal structures.

As is the case for many of the large calixarene crystal structures, diffraction data are sometimes quite weak, and the amount of solvent of crystallization should be taken as approximate. In the figures minor disorder components are omitted.

For **1·4.5MeCN**: The entire ^{t}Bu group at atoms C(7), C(40), C(51), C(62), C(7A), C(18A), C(40A) and C(62A) were modelled as disordered over two sets of positions with major occupancies 68.3(15)%, 71.4(17)%, 63(2)%, 63.1(14)%, 68(4)%, 68(2)%, 74.3(14)% and 59(2)%, respectively. The chloride ion Cl(2A) was modelled as above with a major occupancy of 73(5)%. Platon squeeze recovers 47 electrons in one void of 111 Å^3, giving 2 extra MeCNs per unit cell. The MeCN at N(7) was refined at half weight.

For **2·4MeCN:** Refined as a 2-component twin with major component 54.30(10)%. Components 0.5431:0.4569(10). Component 2 rotated by 8.1802° around [–0.01 0.98 0.18] (reciprocal) or [0.20 0.92 0.33] (direct). 4 MeCNs of crystallisation which lie *exo* to the complex. Two of these are unique. ^{t}Bu group at C(40) was modelled as two-fold disordered with major component occupancy 67.0(15)%. The largest residual electron density peak lies near Cl(2) at the end of the alkyl chain, suggesting some possible unresolved disorder.

For **3·6.5MeCN**: One ^{t}Bu group, at C(62), was modelled as disordered with the methyl groups split over two sets of positions with major occupancy 52.24(9) %. 2.5 MeCNs were modelled as point atoms, with another 1.5 modelled as a diffuse area of electron density by the Platon Squeeze procedure. Squeeze recovered 132 electrons in 4 voids with 33 electrons per void. MeCN has 22 electrons, so 1.5 MeCN per void.

For **4·1.5MeCN**: The whole tBu group at C(18) was modelled as disordered over two sets of positions with major occupancy 67.1(16)%. ^{t}Bu methyl groups at C(73) and C(84) modelled similarly with major occupancy 74.6(16) and 64(4)% respectively. The MeCN group at N(4) was modelled at half weight due to apparent partial occupancy. That at N(3) was fully occupied, so 1.5 molecules of MeCN of crystallisation per metal complex.

For **5·11MeCN:** The methyl groups on the ^{t}Bu groups at C(18), C(62A) and C(84A) were modelled as disordered over two sets of positions with major occupancies 62.4(10)%, 55.5(10)% and 51.6(19)%, respectively. Platon squeeze recovers 355 electrons in 4 voids, giving 16 MeCNs per unit cell or an extra 8 MeCNs per asymmetric unit. This corresponds with point atom observations. The carbon atom C(90), part of the MeCN at N(1), was modelled as disordered over two sets of positions with major occupancy 54(4)%. The carbon atoms C(95A) and C(96A), part of the MeCN at N(4A), were modelled as disordered over two sets of positions with major occupancy 59.2(12)%. The coordinated MeCN ligands, including N(3A) and N(4A) appear rather bent, despite the use of restraints.

For **6·6MeCN**: The methyl groups on the ^{t}Bu groups at C(8), C(40) and C(51) were modelled as disordered over two sets of positions with major occupancies 91.9(5)%, 69.0(7)% and 51.5(6)%, respectively.

For **7·7.5MeCN**: The methyl groups on the ^{t}Bu group at C(7) were modelled as disordered over two sets of positions with major occupancy 67.6(13)%. MeCN including N(9) was modelled as two-fold disordered with atom C(106) common to both components and major site occupation factor 65.4(11)%; while that at N(10) was similarly modelled with C(108) common to both components and major site occupation factor also 65.4(11)%. Platon squeeze recovers 314 electrons in 4 large voids and 4 medium sized voids. Approx. 3 MeCNs in each large void and ½ an MeCN in each medium void giving 14 additional MeCNs per unit cell or an extra 3.5 MeCNs per Ti_3 complex. This corresponds with point atom observations.

For **8·14MeCN**: The methyl groups on the ^{t}Bu groups at C(7), C(29), C(52) and their symmetry-related atoms, were modelled as disordered over two sets of positions with major occupancies 63(2)%, 60(5)% and 62.2(12)% respectively. The entire ^{t}Bu group at atoms C(18) and C(85) was modelled as stated above with major occupancies 57.46(12)% and 63.8(12)%, respectively. Platon squeeze recovers 291 electrons in 2 voids, giving 14 MeCNs per unit cell or an extra 7 MeCNs per Ti_8 complex. This corresponds with point atom observations. There are 6 MeCNs coordinated to Na ions, of which that at N(5) was refined at half weight. There are two non-coordinated MeCNs refined as point atoms, of which that at N(7) was refined at half weight.

For **9·7MeCN**: The methyl groups on the ^{t}Bu groups at C(73) and C(117) were modelled as disordered over two sets of positions with major occupancies 60(3)% and 71.1(10)%, respectively. Platon squeeze recovers 332 electrons in 8 voids, giving 16 MeCNs per unit cell or an extra 4 MeCNs per Ti_8 complex. This corresponds with point atom observations.

For **10·15.5MeCN**: The entire ^{t}Bu group at atom C(18) was modelled as disordered over two sets of positions with major occupancy 62(3)%. The methyl groups on the ^{t}Bu groups at C(51), C(62), C(84), C(117), C(150), C(183) and C(293) were modelled as disordered over two sets of positions with major occupancies 64(1)%, 61(1)%, 59.8(10)%, 69(1)%, 64(1)%, 58(1)% and 54(4)%, respectively. The carbon atoms C(363) and C(364), part of the MeCN at N(6), were modelled as disordered over two sets of positions with major occupancy 54(2)%. The carbon atoms C(367) and C(368), part of the MeCN at N(8), were modelled as disordered over two sets of positions with major occupancy 60(2)%. Platon squeeze recovers 177 electrons in 1 void, giving 8 MeCNs per unit cell. The sodium ion(s) labelled Na(2), Na(3), and Na(4) were modelled as disordered over three sets of positions with occupancies 52(2)%, 19.2(9)% and 29(1)%, respectively, with occupancies restrained to sum to a single Na ion required for charge balance.

For **11·7.25CH_2Cl_2**: The whole ^{t}Bu group at C(7) and C(84) were modelled as disordered over two sets of positions with major occupancies 55.4(19)% and 50.5(17)%, respectively. The methyl groups on the ^{t}Bu group at C(51) were modelled as disordered over two sets of positions with major occupancy 51.1(18)%. Platon squeeze recovers 222 electrons per unit cell in eight voids; DCM has 42 electrons so five extra DCMs per unit cell.

For **12·hexane**: The ^{t}Bu group at C(11) was modelled as having the methyl groups disordered over two set of positions with major occupancy 81.8(8)%. Atoms C(19) and C(20) were modelled as 2-fold disordered in the hexane molecule with major component occupancy 67.0(7)%.

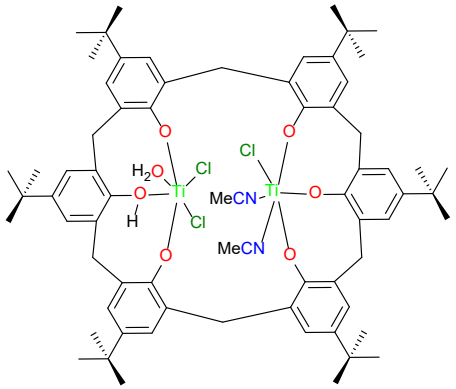

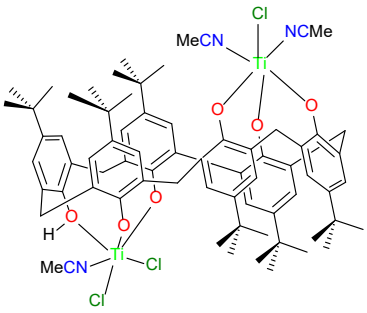

$[Ti_2Cl_3(MeCN)_2(OH_2)(L^1H)][Ti_2Cl_3(MeCN)_3(L^1H)]\cdot 4.5\ MeCN$ (**1**·4.5MeCN)

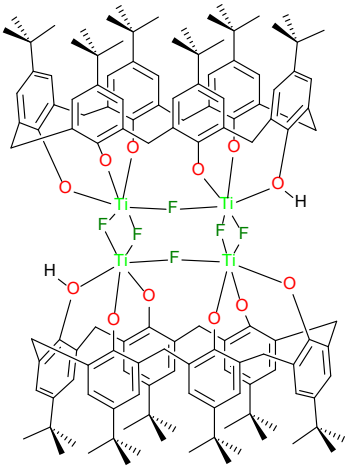

$[(TiF)_2(\mu\text{-}F)L^1H]_2\cdot 6.5MeCN$ (**3**·6.5MeCN)

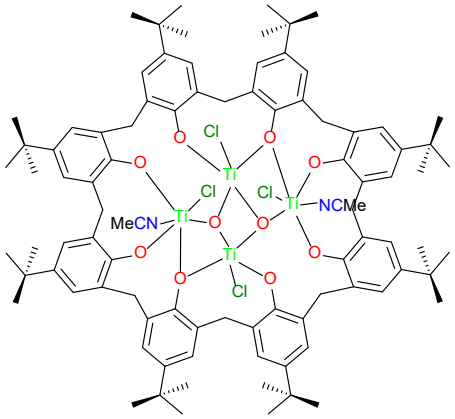

$[(TiCl)_2(TiClNCMe)_2(\mu_3\text{-}O)_2(L^2)]\cdot 1.5MeCN$ (**4**·1.5MeCN)

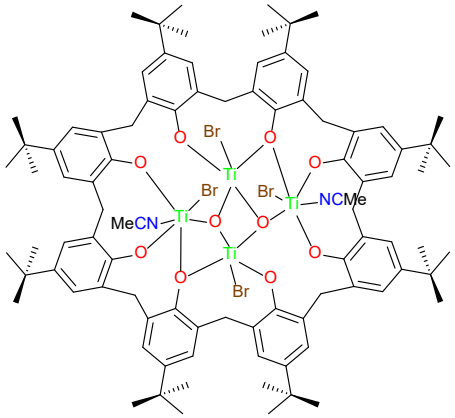

$[(TiBr)_2(TiBrNCMe)_2(\mu_3\text{-}O)_2(L^2)]\cdot 6MeCN$ (**6**·6MeCN)

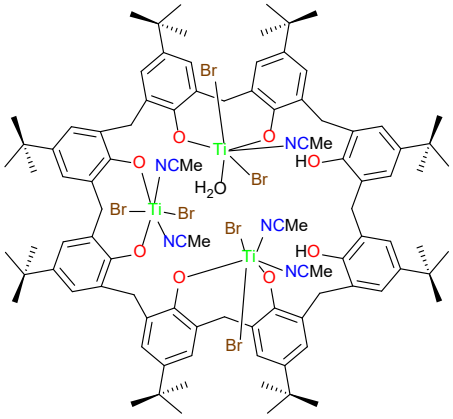

$[Ti(NCMe)_2Br_2][Ti(O)Br_2(OH_2)(NCMe)](L^2H_2)\cdot 7.5MeCN$ (**7**·7.5MeCN)

Figure S1. Titanocalix[6 and 8]arene complexes **1**, **3**, **4**, **6** and **7**.

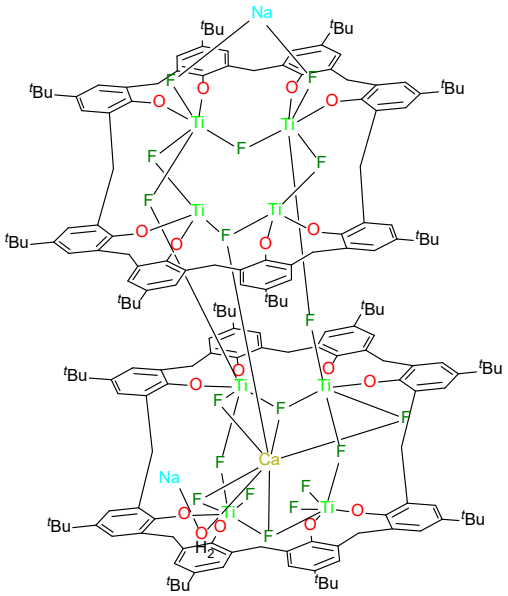

$[(Ti_8CaF_{20}(OH_2)Na_2(MeCN)_4)(L^2)_2]\cdot 14MeCN$ (**8**·14MeCN)

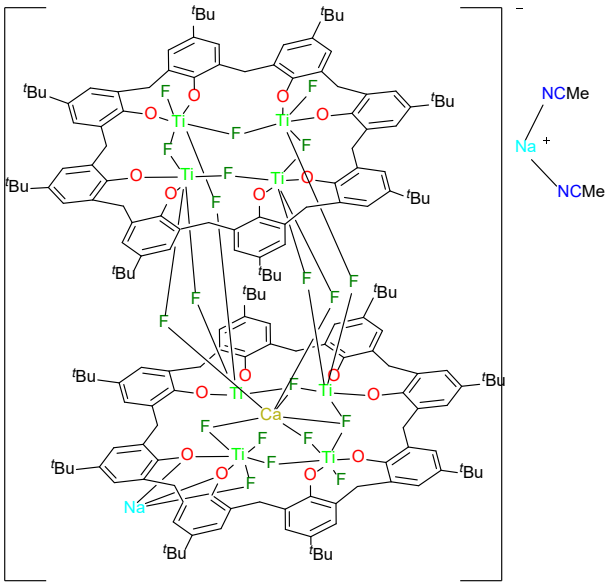

$[Na(MeCN)_2][Ti_8CaF_{20}NaO_{16}(L^2)_2]\cdot 7MeCN$ (**9**·7MeCN)

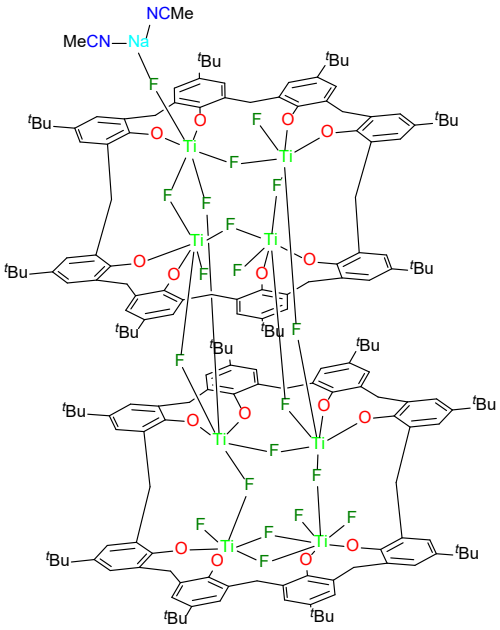

$[Na]_6[Ti_8F_{20}Na(MeCN)_2(L^2)]\cdot[Ti_8F_{20}Na(MeCN)_{0.5}(L^2)]\cdot 15.5(MeCN)$ (**10**·15.5MeCN)

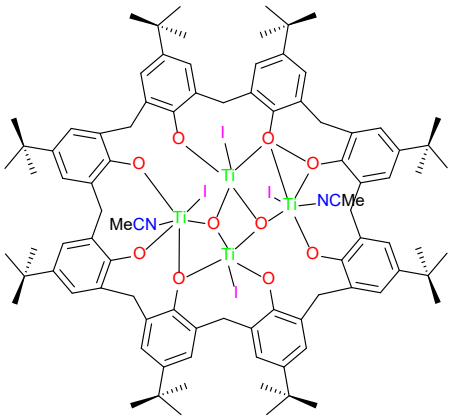

$[(TiI)_2(TiINCMe)_2(\mu_3\text{-}O)_2(L^2)]\cdot 7.25\ CH_2Cl_2$ (**11**·7.25CH_2Cl_2)

Figure S2. Titanocalix[8]arene complexes **8-11**.

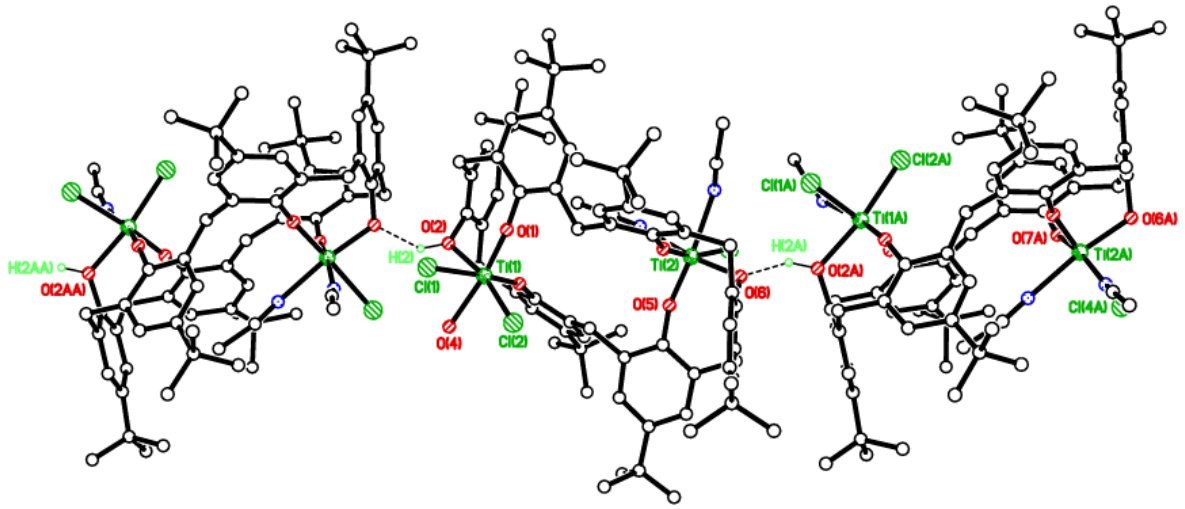

Figure S3. H-bonded, zig-zag chains of **1**, in the *b*-direction.

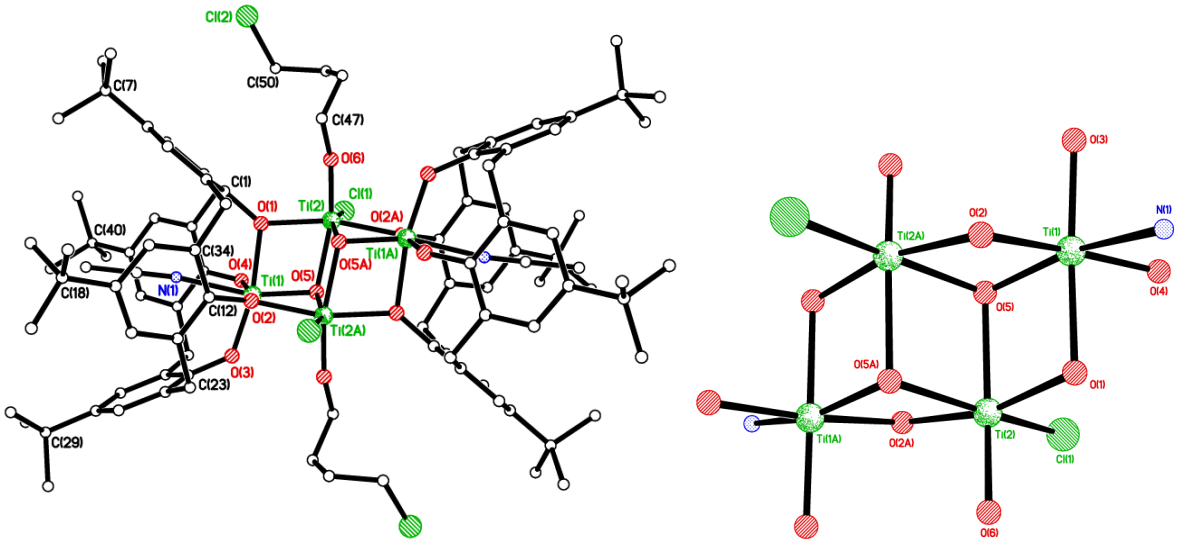

(a) **(b)**

Figure S4. Molecular structure (a) and core (b) of $[Ti_4Cl_2(\mu_3\text{-}O)_2(NCMe)_2(L)_2(O(CH_2)_4Cl)_2]\cdot 4MeCN$ (**2**·4MeCN). Solvent of crystallization and H atoms omitted for clarity. Selected bond lengths (Å) and angles (°): Ti(1)–O(1) 2.071(2), Ti(1)–O(2) 2.065(2), Ti(1)–O(3) 1.848(2), Ti(1)–O(4) 1.826(2), Ti(1)–O(5) 1.840(2), Ti(1)–N(1) 2.221(3), Ti(2)–O(1) 1.988(2), Ti(2)–O(2A) 2.022(2), Ti(2)–O(5) 2.077(2), Ti(2)–O(5A) 2.028(2), Ti(2)–O(6) 1.771(2), Ti(2)–Cl(1) 2.3142(8); O(1)–Ti(1)–O(2) 84.26(8), O(1)–Ti(1)–O(3) 166.44(9), O(2)–Ti(1)–O(4) 165.67(9), O(1)–Ti(2)–O(2A) 165.94(9), Ti(2)–O(5)–Ti(2A) 102.37(9), O(5A)–Ti(2)–Cl(1) 96.00(6). Symmetry operator A = –x+1, –y+1, –z.

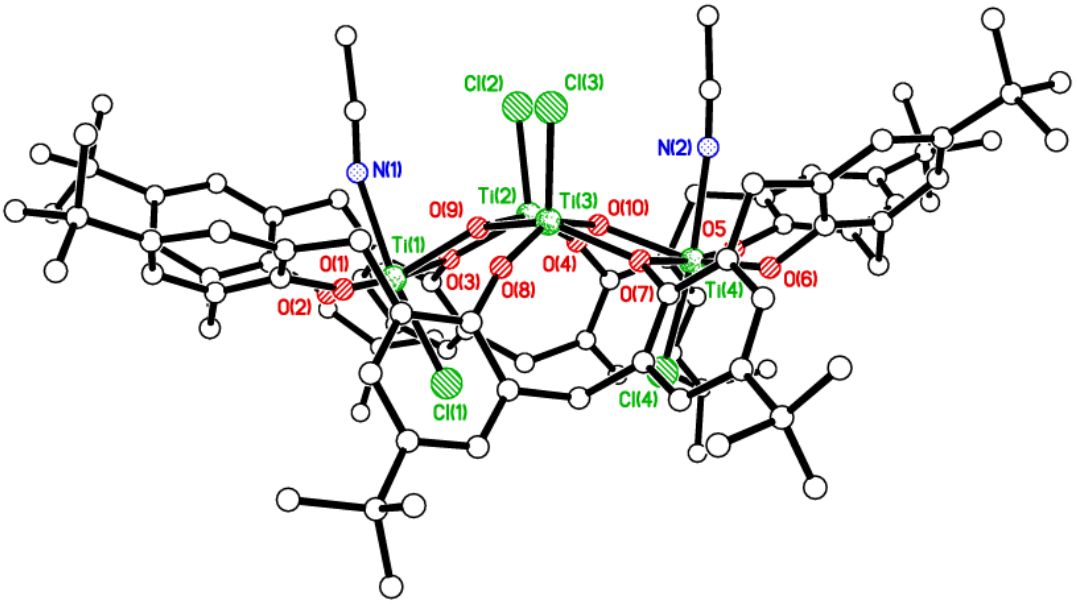

Figure S5. Alternative view of $[(TiCl)_2(TiClNCMe)_2(\mu_3\text{-}O)_2(L^2)]\cdot 1.5MeCN$ (**4**·1.5MeCN)

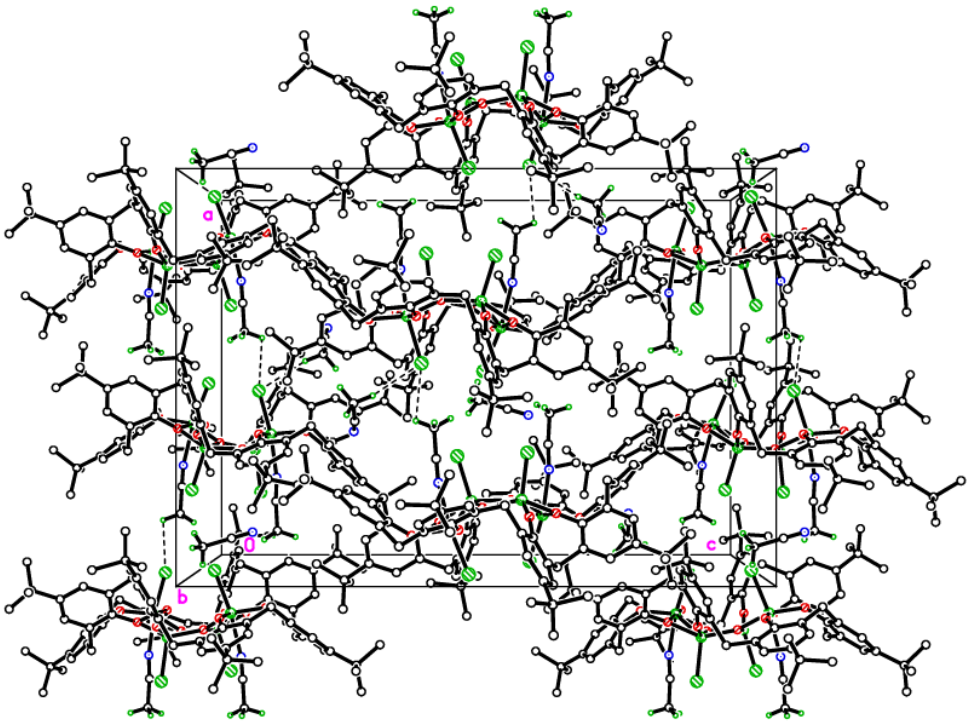

Figure S6. C–H···Cl weak intermolecular interactions in **4** parallel to *a*.

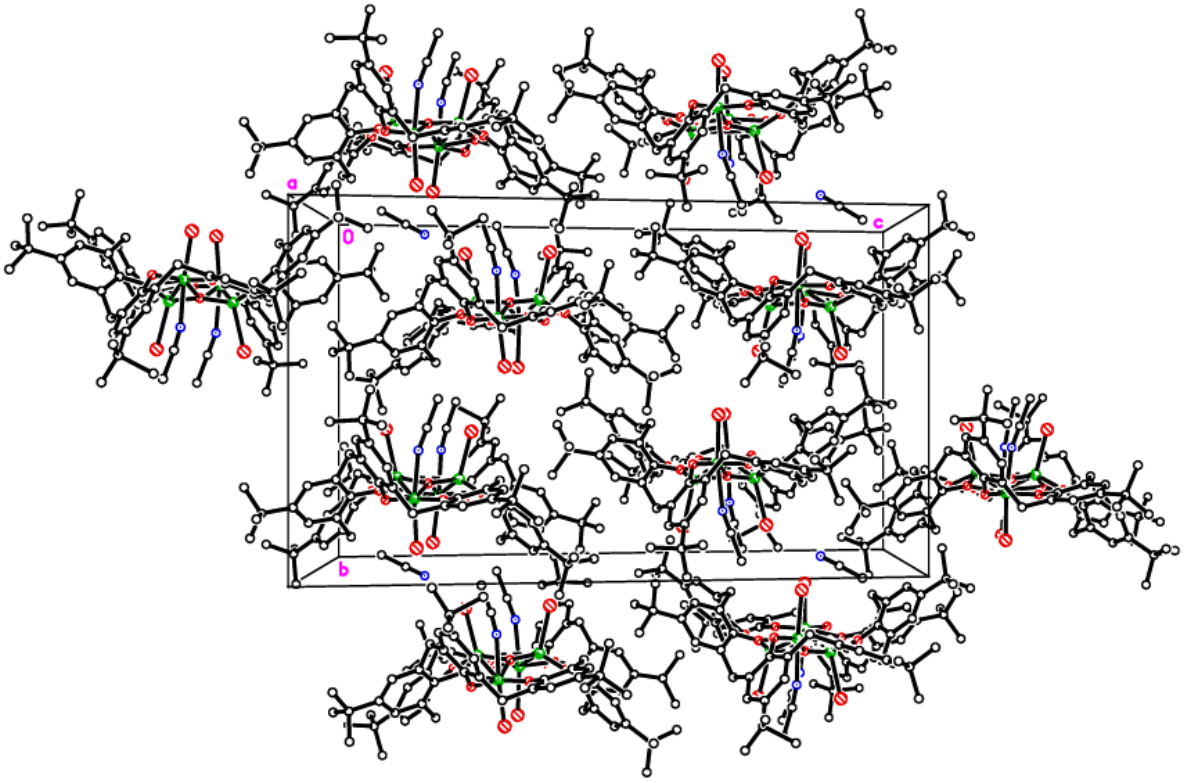

Figure S7. View of the layers of molecules of **6**.

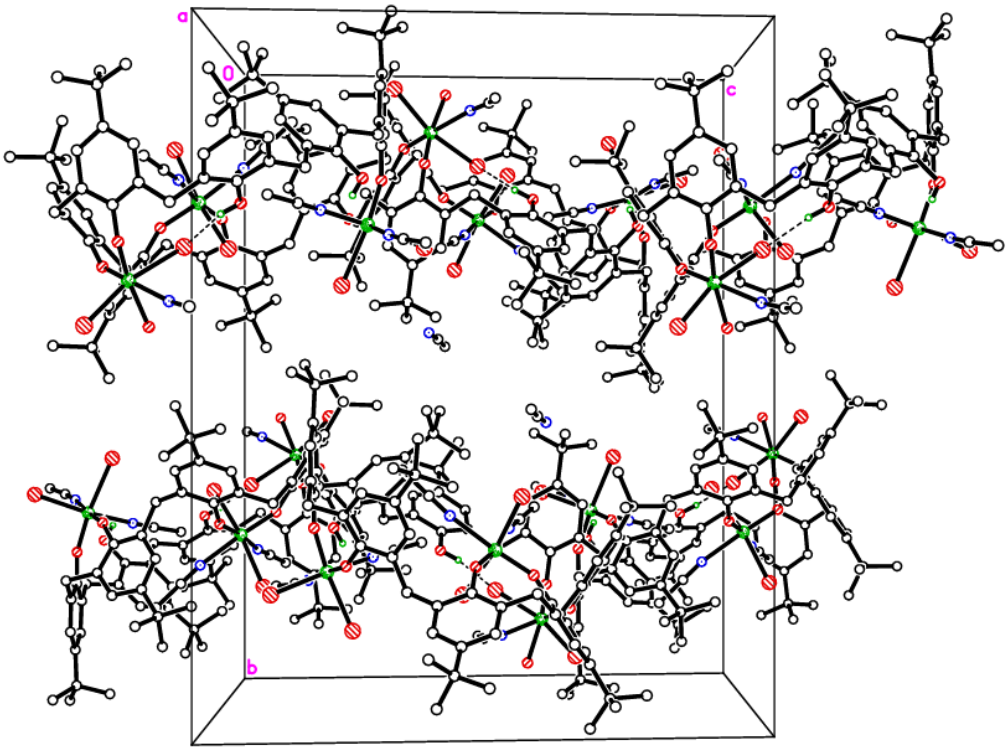

Figure S8: Molecules of **7** are arranged in an undulating layer structure in the *a*/*c* plane.

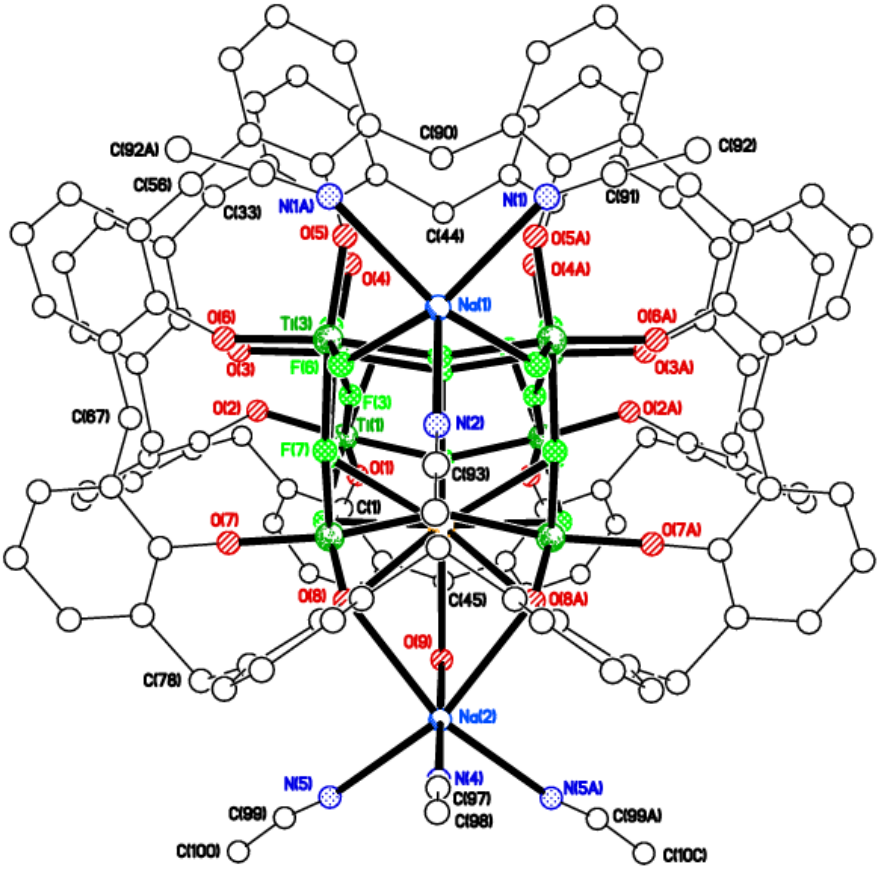

Figure S9: Alternative view of **8**.

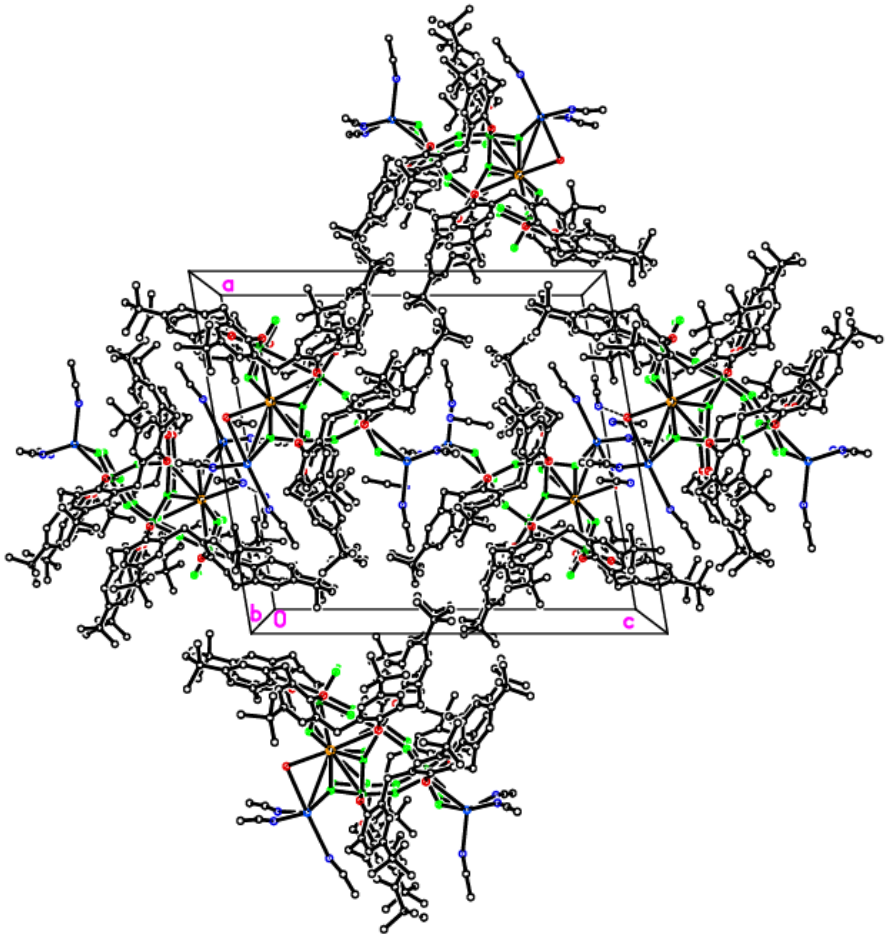

Figure S10: View of **8** perpendicular to b/c plane.

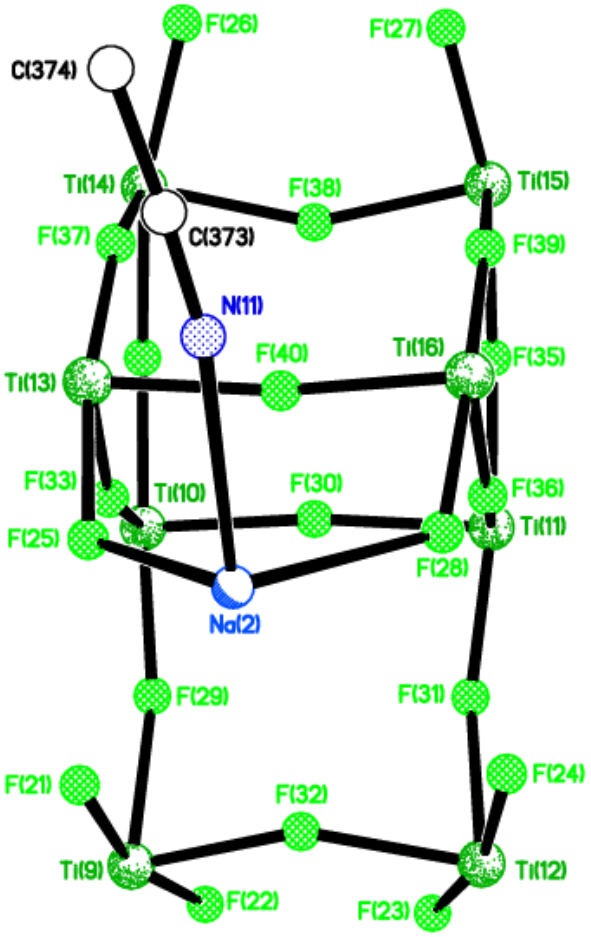

Figure S11: Alternative view of the core of **10**.

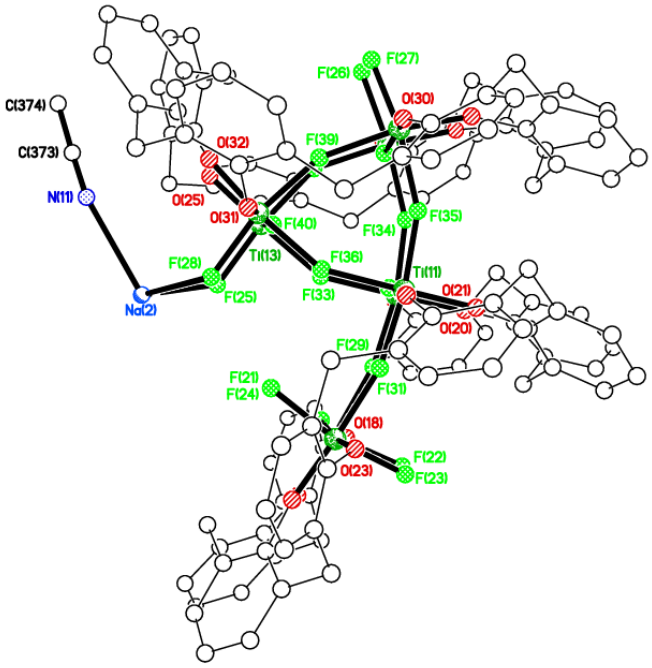

Figure S12: Side-on view of partial calixarene stacking in **10**.

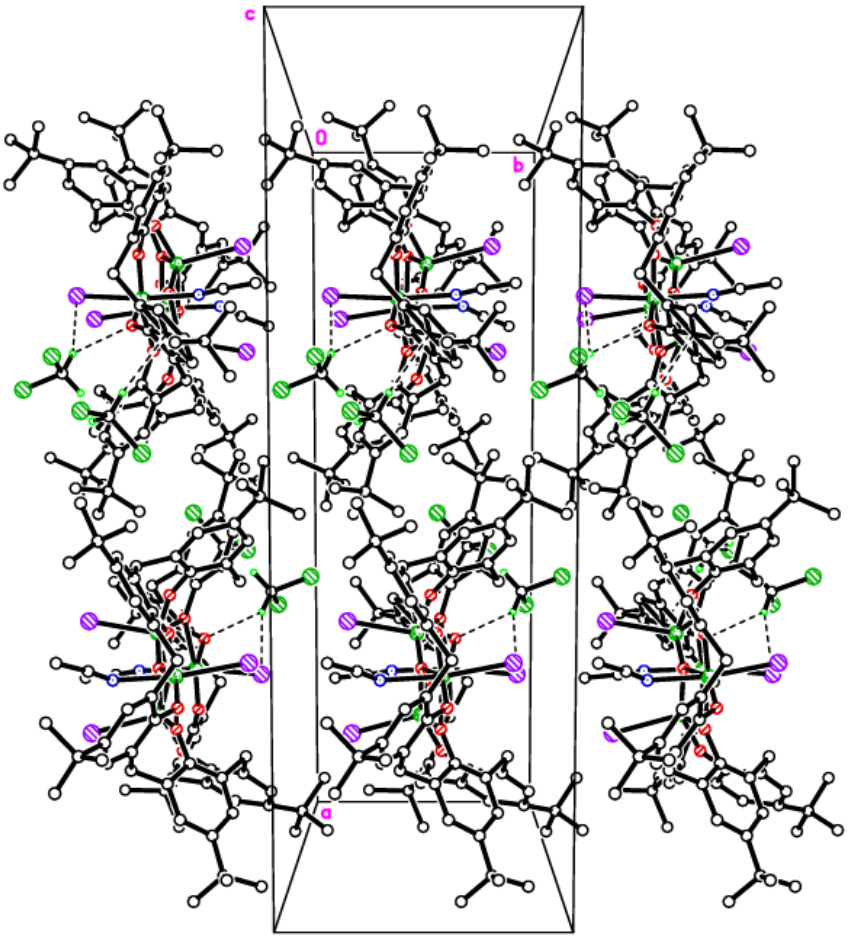

Figure S13: Layers of molecules of **11** in the *a*/*c* plane.

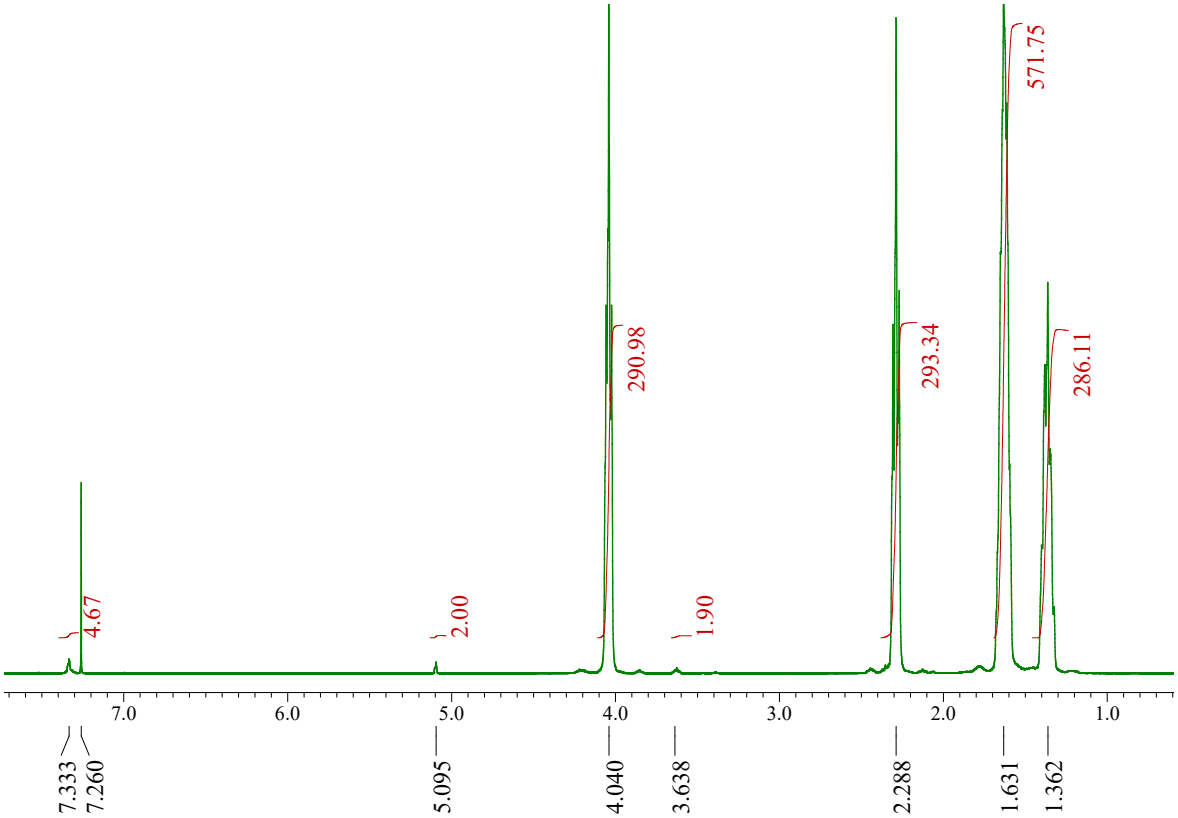

Figure S14. ^{1}H NMR spectrum ($CDCl_3$, 400 MHz, 298 K) of the PCL synthesized in Table 1, entry 16.

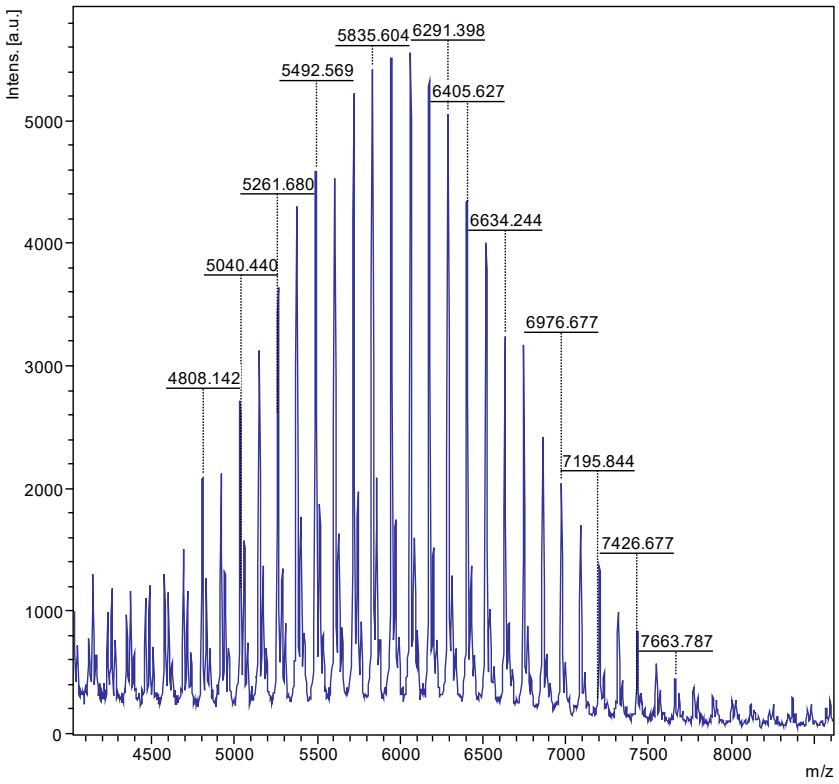

Figure S15. MALDI-ToF spectrum of the PCL synthesized in Table 1, entry 16.

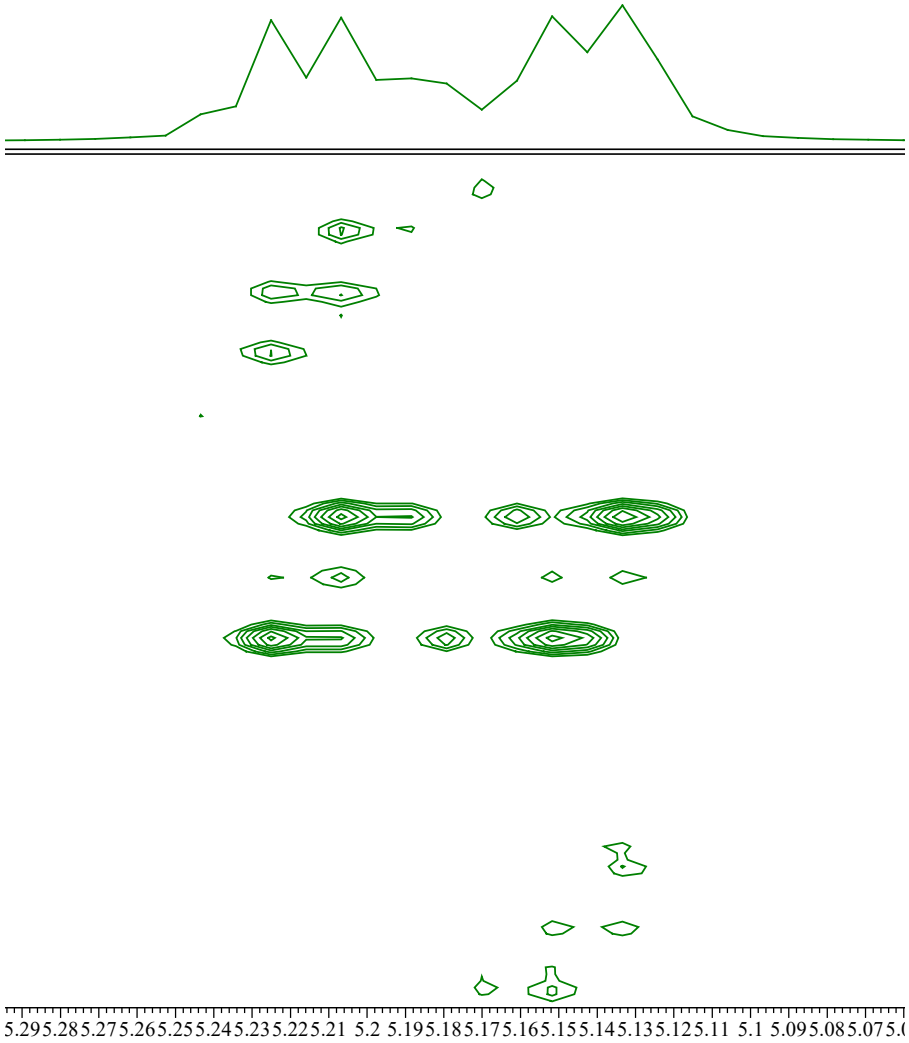

Figure S16: 2D *J*-resolved ^{1}H NMR spectrum ($CDCl_3$, 400 MHz, 298 K) of the PLA synthesized using **1**.

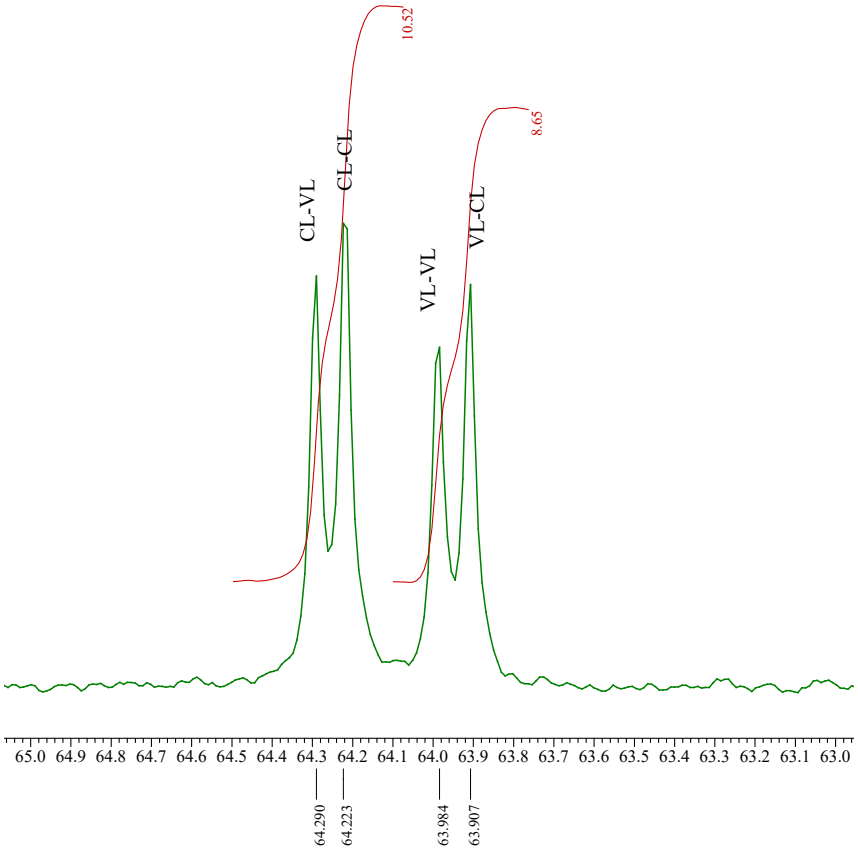

Figure S17: ^{13}C NMR spectrum ($CDCl_3$, 400 MHz, 298 K) of the CL-VL Copolymer synthesized with **10** (65-63 ppm).

Equation S1: Determination of number-average sequence length for CL. [1]

$$L_{CL} = \frac{(I_{CL\text{-}CL})}{(I_{VL\text{-}CL})} + 1$$

Where $I_{CL\text{-}CL}$ and $I_{VL\text{-}CL}$ is the area of the peak belonging to the CL-CL and VL-VL dyad, respectively.

Equation S2: Determination of number-average sequence length for VL. [1]

$$L_{VL} = \frac{(I_{VL\text{-}VL})}{(I_{CL\text{-}VL})} + 1$$

Where $I_{VL\text{-}VL}$ and $I_{CL\text{-}VL}$ is the area of the peak belonging to the VL-VL and CL-VL dyad, respectively.

Equation S3: Determination of the Randomness Character (R). [1]

$$R = \frac{1}{L_{CL}} + \frac{1}{L_{VL}}$$

Completely block Copolymers: R = 0
Copolymers with a “blocking” tendency: R < 1
Completely random copolymers: R = 1
Copolymers with an alternating tendency: R >1
Completely alternating copolymers: R = 2

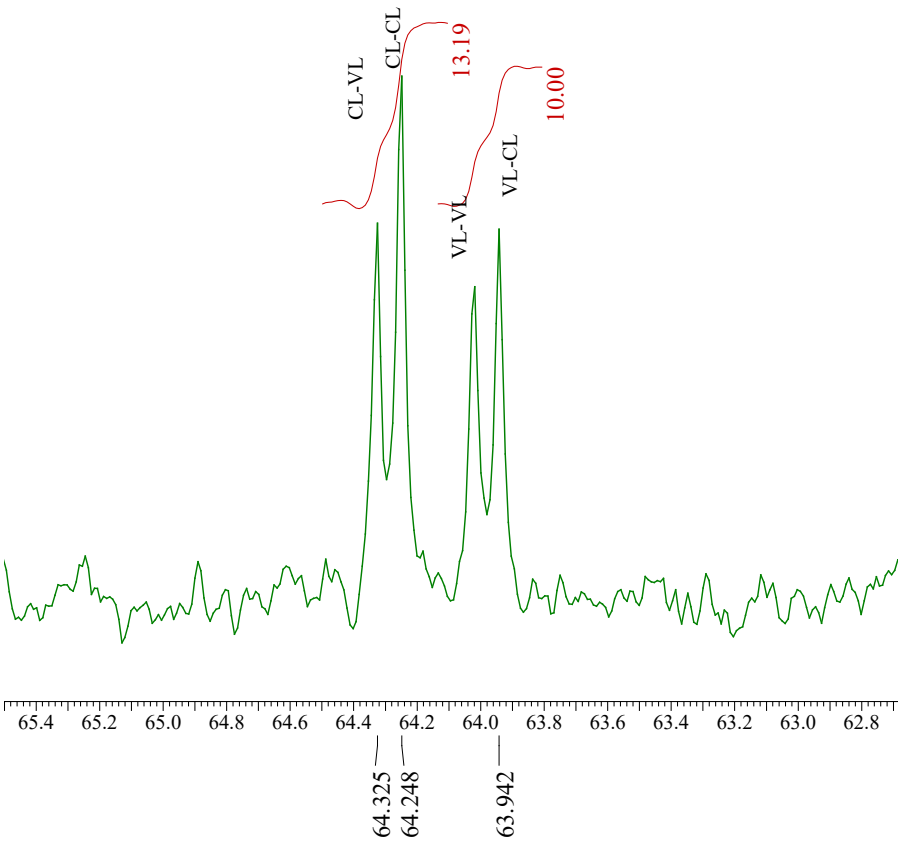

Figure S18: ^{13}C NMR spectrum ($CDCl_3$, 400 MHz, 298 K) of the CL-VL Copolymer synthesized with **11** (65-63 ppm).

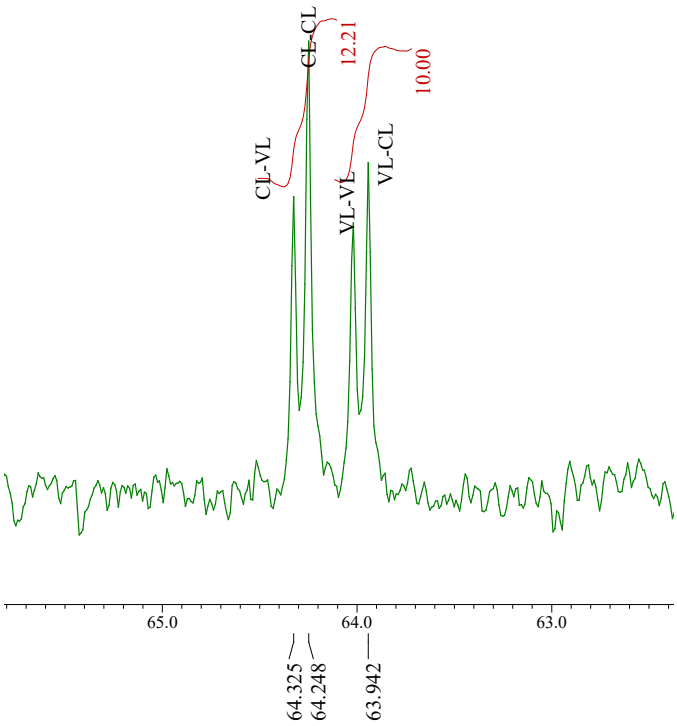

Figure S19: ^{13}C NMR spectrum ($CDCl_3$, 400 MHz, 298 K) of the CL-VL Copolymer synthesized with **12** (65-63 ppm).

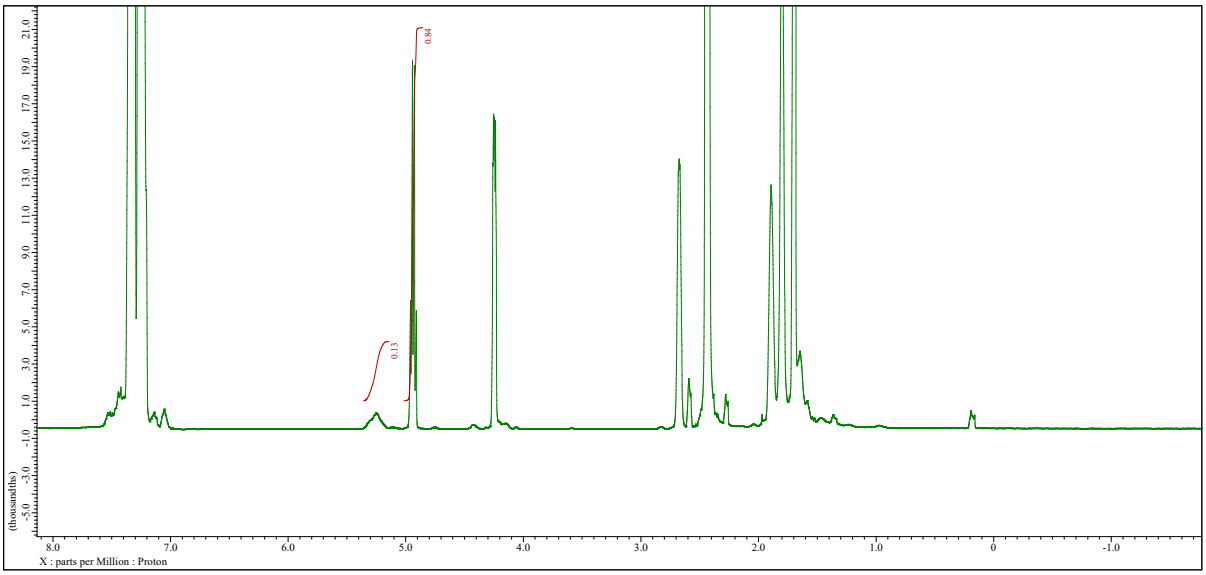

Figure S20: ^{1}H NMR spectrum ($CDCl_3$, 400 MHz, 298 K) of the crude ε–CL/*r*-LA co-polymerization mixture synthesized with **1**.

References

[1] (a) Q. Hu , S.-Y. Jie, P. Braunstein and B.-G. Lia *Chinese J. Polym. Sci*. 2020, **38**, 240–247; (b) M. A. Woodruff and D. W. Hutmacher *Prog. Polym. Sci.* 2010, **35**, 1217−1256; (c) T. Wu, Z. Wei, Y. Ren, Y. Yu, X. Leng and Y. Li *Polym. Degrad. Stab*. 2018, **155**, 173−182; (d) M. T. Hunley, N. Sari, and K. L. Beers, *ACS Macro Lett.* 2013, **2**, 375−379.